

FREQUENCY RECONFIGURABLE USING CLRH FOR 5G SUB-6 GHz WIRELESS APPLICATION

Marwa M. Ismail¹, Bashar Bahaa Qas Elias², Bashar S. Bashar³, Taha A. Elwi⁴, Z. A. Rhazali⁵, Halina Misran⁶

^{1,2} Department of Information and Communication Engineering, College of Information Engineering, Al-Nahrain University, Jadriya, Baghdad, Iraq

^{3,5,6} Department of Electrical and Electronic Engineering, College of Engineering, Universiti Tenaga Nasional, Kajang, Malaysia

⁴ Department of Automation and Artificial Intelligence Engineering, College of Information Engineering, Al-Nahrain University, Jadriya, Baghdad, Iraq

nareenem@nahrainuniv.edu.iq¹, bashar.bahaa@nahrainuniv.edu.iq², PE21173@student.uniten.edu.my³, taelwi82@gmail.com⁴, zetiakma@uniten.edu.my⁵, halina@uniten.edu.my⁶

Corresponding Author: **Halina Misran**

Received:29/04/2025; Revised:15/06/2025; Accepted:09/12/2025

DOI:[10.31987/ijict.8.3.330](https://doi.org/10.31987/ijict.8.3.330)

Abstract- This paper presents a flexible and adjustable antenna design that reduces interference in different practical applications. The antenna, shaped like a square with slots and integrated pin diodes, enables frequency adjustment by connecting or disconnecting components. Made of certain substrate material, the antenna operates at five frequency bands commonly used in 5G sub-6 GHz applications. Along with improving the connection with the Metamaterial (MTM) structure by using four PIN diodes without altering the radiation pattern, the new design replaces the via with a fractal technique, which cuts down on energy losses and boosts performance while also lowering costs. Simulation results demonstrate excellent impedance matching, multiple adjustable bands, and significant gain(>10 dBi). The antenna exhibits radiation patterns and achieves an efficiency greater than 75%. Analysis under various conditions shows the antenna's performance on curved surfaces, making it suitable for adaptable electronic systems. A comparison with prior studies highlights the antenna's potential within the specified frequency ranges.

keywords: MTM, Reconfiguration, Beam splitting, Hilbert, Taconic FR-30.

I. INTRODUCTION

The rapid transition in wireless communications technology in recent years is essential due to an increasing demand for multiple wireless services within the device [1]. Unfortunately, traditional antennas have proven inadequate for meeting the requirements of modern wireless communication systems [2]. Consequently, antennas that can adapt their characteristics based on the surrounding environment are now reconfigurable [3]. Moreover, reconfigurable antennas designed for wireless systems operating at varying frequencies are crucial in fulfilling the new system requirements [4]. The primary feature of these antennas is represented in their ability to generate high return losses (S11), although they are not sufficiently effective in producing high gain and broad bandwidth [5]. Over the years, researchers have attempted to address these constraints by altering the shape and size of the patch element and ensuring proper impedance matching [6]. The inset feed technique is utilized for optimal impedance matching [7]. The feeding location and techniques significantly impact impedance matching, consequently influencing antenna performance parameters [8].

The paper presents a microstrip antenna with a rectangular geometry integrated with PIN diodes to allow for operation at different resonating frequencies [9]. The antenna utilizes an inset feeding technique and requires specific DC biasing

circuitry to control the PIN diodes. The appropriate DC biasing circuit ensures proper isolation, necessary biasing, and reliable switching performance. The final antenna design also includes two small square patches connected through PINs. Detailed analysis of the PIN diodes in both ON and OFF states is conducted under assumed proper biasing conditions [10]. All simulations are performed using CST Studio. The upcoming sections will delve into the antenna design and its characteristics.

II. ANTENNA DESIGN

This section presents the geometric specifications and outlines the theoretical framework employed in developing the final design of the reconfigurable multiband antenna. The frequency reconfiguration is achieved with pin diodes' CLRH equivalent circuit. The proposed antenna modifies its performance by altering the states of the pin diode (on/off), leading to resonance at various frequency bands with favorable gain and return loss characteristics, detailed subsequently [11].

A. Antenna Geometry

Through the proposed design in this work displayed in Fig.1 and Fig. 2, respectively, the selection of a good substrate material is required, as this provides the capacitive effect. Material like Taconic RF-30 (Lossy) is a frequently used substrate [5]. Here, Taconic RF-30 (Lossy) substrate thickness (h) of 1.6 mm, loss tangent, and relative permittivity of 4.3 are used. Full rectangular with slot patch is designed with a width of 99.03 mm and length of 69.61 mm. The antenna feed must be designed in a way that it must be capable of achieving good impedance matching. The power line also plays an important role in antenna performance at high frequencies [12]. The power line should have an impedance equal to the antenna's characteristic impedance for best results. A coaxial cable is used to feed the antenna, connecting to a point within the patch where the input impedance is 50Ω [13]. The various formulas used to design such an antenna are expressed in Table I.

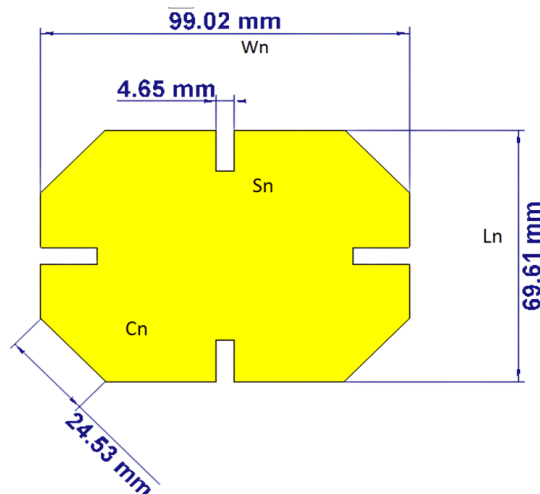


Figure 1: Antenna Geometry.

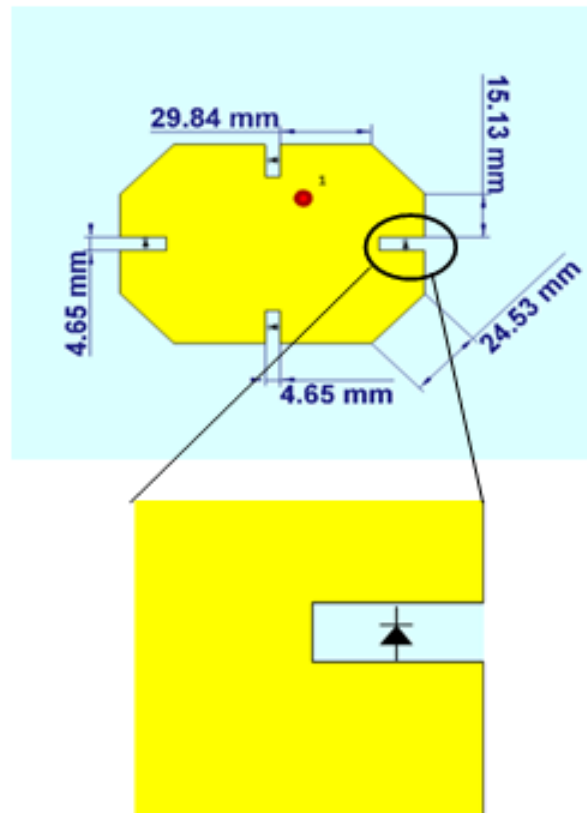


Figure 2: Geometry of the Antenna with Pin Diode.

TABLE I
 Parameter values

PARAMETERS	VALUE (mm ²)
WN	99.02
LN	69.61
SN	4.65
CN	24.53

B. Reconfiguration Process

The reconfiguration process involves the etching of T-shaped slots on either side of a truncated patch; each slot occupies an area equal to 1 mm² and is used to insert the PIN diode [14]. Fig. 3 shows an equivalent circuit model for PIN diode-based reconfiguration in ON and OFF states and a value for the lumped element (R, L, C). From among the seven cases, six of them are chosen [15]. It modifies a surface current distribution across structures by changing the pin diode state, which affects antenna performance [16].

This proposed antenna has nine different operating modes that are good enough. These resonant modes' details and their corresponding PIN states are listed in Table II.

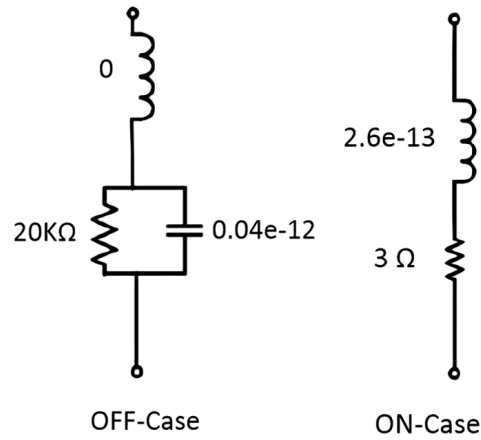


Figure 3: RLC circuit mode using Pin-diode.

TABLE II
 Proposed Antenna Using PIN Diode

Case	PIN Diode				Frequency (GHz)
	A1	A2	A3	A4	
Case 1	OFF	OFF	OFF	OFF	2, 2.3, 3.3, 4.6, 4.8
Case 2	OFF	OFF	OFF	ON	2, 3.3, 4.6, 4.8, 5, 5.6
Case 3	OFF	ON	OFF	ON	2, 2.3, 2.4, 3.5, 3.6, 4.6, 5, 5.6
Case 4	ON	OFF	OFF	ON	1.4, 2.2, 2.5, 4.6, 4.8, 5, 5.6
Case 5	ON	OFF	ON	OFF	1.4, 2.5, 3.3, 3.5, 4.6, 4.8
Case 6	ON	ON	OFF	ON	1.4, 2.1, 2.3, 2.5, 4.6, 5, 5.6, 6
Case 7	ON	OFF	ON	OFF	2.1, 2.5, 2.6, 3.2, 3.7, 4.1, 5.2, 5.4
Case 8	ON	ON	ON	OFF	2.2, 2.6, 4.6, 5, 5.6

Upon the Eq. (1), a rectangular patch antenna can be made frequency reconfigurable by introducing a slot and placing a PIN diode across it. The diode acts as a switch that changes the path of the current and thus the effective electrical length of the antenna. In the ON state (forward bias), the diode offers low resistance, allowing the current to flow uninterrupted, maintaining the original resonant frequency.

$$f_r = \frac{c}{2L\sqrt{\epsilon_{\text{eff}}}} \quad (1)$$

where L is the patch length and ϵ_{eff} is the effective permittivity. In the OFF state (reverse bias), the high resistance of the diode forces the current to flow around the slotted PIN, increasing the effective length to $(L + \Delta L)$ and thus lowering the

resonant frequency, as demonstrated in Eq.(2).

$$f_{\text{new}} = \frac{c}{2(L + \Delta L)\sqrt{\epsilon_{\text{eff}}}} \quad (2)$$

Next, the diode resistance is modeled based on the Eq. (3) and Eq. (4), respectively.

$$Z_{\text{ON}} = R_f + j\omega L_s \quad (3)$$

$$Z_{\text{OFF}} = R_r + \frac{1}{j\omega C_j} \quad (4)$$

Where R_f , R_r , L_s , and C_j are its parasitic parameters. A biasing circuit using a choke (for RF shielding) and a DC-isolating capacitor (for DC isolation) ensures proper diode control without disrupting the radiation. The input impedance of the antenna is adjusted using the transmission line theorem presented in Eq. (5).

$$Z_{\text{in}} = Z_o \cdot \frac{Z_L + jZ_o \tan(\beta d)}{Z_o + jZ_L \tan(\beta d)} \quad (5)$$

Where Z_{in} is the input impedance at a distance d from the load, Z_o is the characteristic impedance of the transmission line, Z_L is the load impedance, β is the phase constant, and d represents the length of the transmission line. This method allows dynamic frequency tuning while maintaining radiation efficiency.

C. CRLH

The proposed CRLH unit cell, see Fig. 4 (a), consists of LH components represented by interdigital capacitor CIDC and stub inductor LTS. The individual CIDC contains four fingers on each side to create a series capacitor with a shunt LTS. Vias are replaced with the Minkowski Fractal inclusions [17]. The advantage of introducing the Minkowski fractal is to minimize the tripped energy in the antenna ground plane with minimum conduction losses, which effectively equalizes the ground plane's capacitive parts, reducing the antenna loss [18].

However, parasitic effects could occur due to introducing these structures, provided by RH components that minimize the antenna gain-bandwidth products. The structure of the CRLH model is shown in Fig. 4 (b). The return loss performance of a fractal antenna with a PIN diode switching and a CRLH structure operating in the 1-6 GHz range is displayed in Fig. 5. In the off state (original design), the antenna exhibits resonances at specific frequencies, indicating good impedance matching. When the PIN diode is turned on, the return loss curve changes, revealing the ability to adjust the frequency by adding new resonances or altering preexisting ones. Compact multiband operation is made possible by the CRLH metamaterial, while bandwidth is improved by the fractal structure. Dynamic tuning is made possible by this design for uses like adaptive wireless systems. The graph demonstrates effective on/off switching at the targeted frequencies with very little reflection loss.

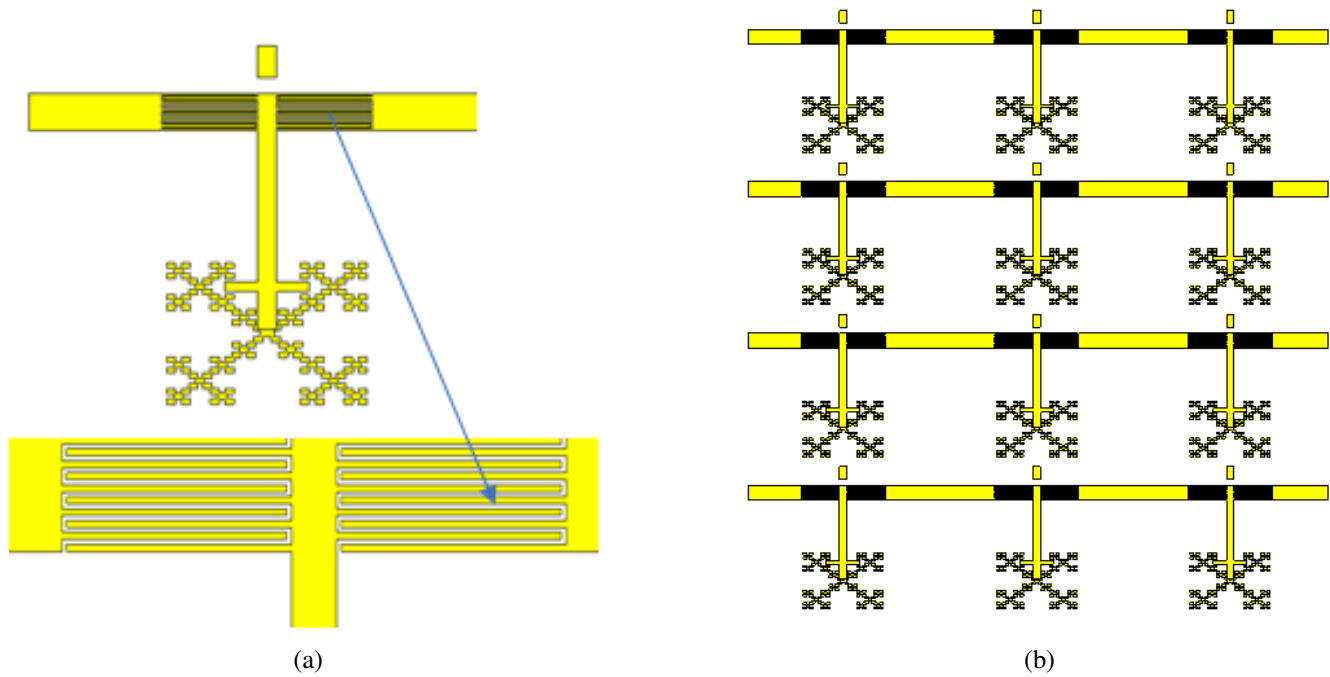


Figure 4: CRLH antenna (a) CRLH (b) overall design structure.

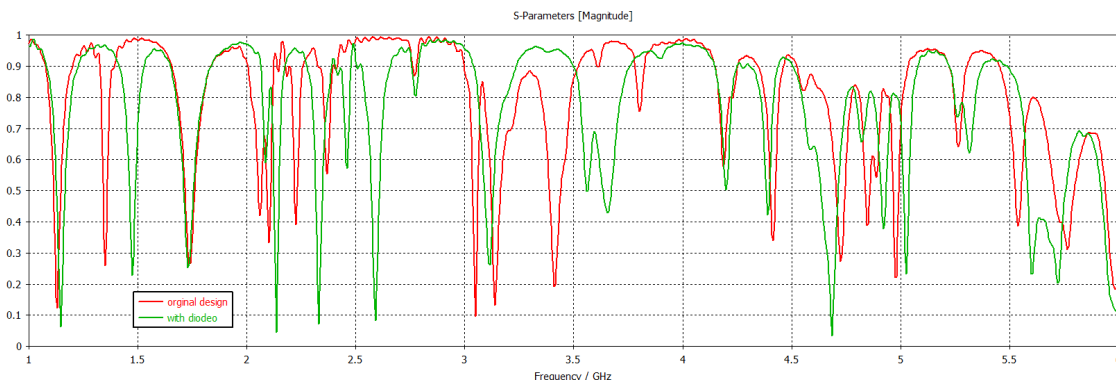


Figure 5: Return loss results at the ON/OFF states (dimensionless).

D. The catamenial design with patch antenna

Fig. 6 (a) depicts the dimensions of the MTM antenna design and then notes when the final design is completed with a patch antenna (see Fig.6 (b)). The simulation gain results are illustrated in Table III, and it's observed that the maximum gain of 12.3 dBi and 7.2 dBi at frequencies 4.6 GHz and 5.6 GHz are achieved.

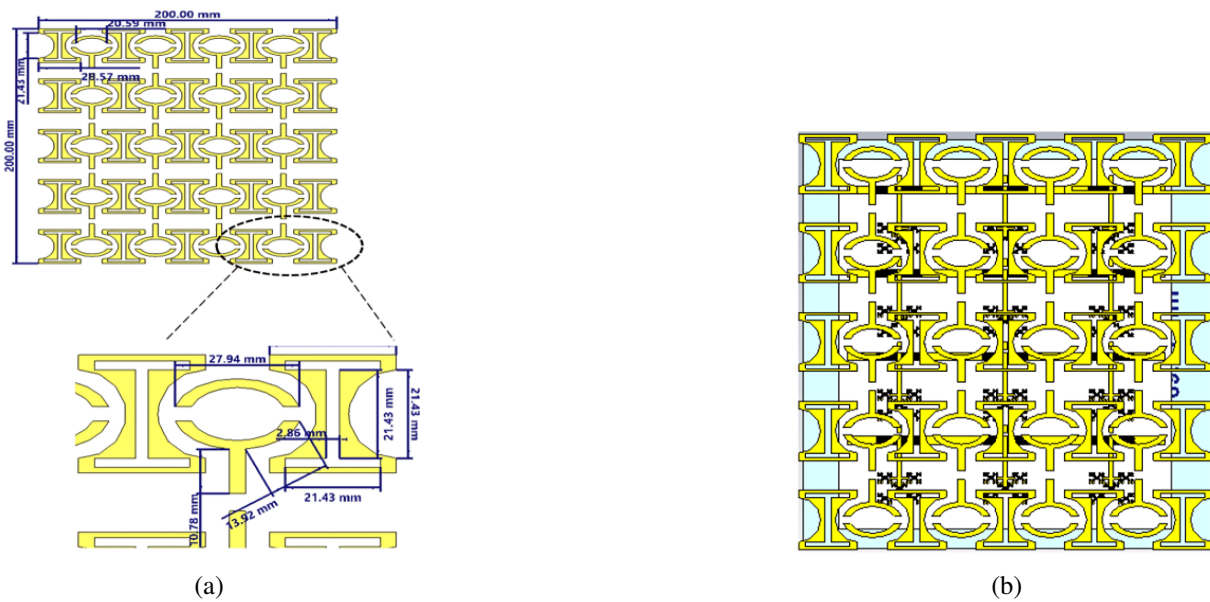


Figure 6: The metamaterial design proposal (a) the MTM structure (b) the MTM with CRLH antenna.

III. RADIATION PATTERN RESULTS

In addition, the resonance frequency and bandwidth, monitored and controlled by the state of the switchable slot, are studied in Fig. 7, Fig.8, and Fig. 9, respectively. In Fig. 7 (a), the radiation pattern at the OFF state resonates at 1.3 GHz and represents a directed single beam. However, in the ON state, the resonance frequency shifts to 1.4 GHz with the main beam shifting to the right directive, as shown in Fig. 7 (b). In the OFF state, the original beam splits into two beams at a frequency of 4.7 GHz. In the ON state, the beam shifts in the left direction at a frequency of 4.6 GHz. At this point, the beam splitting remains the same as the proposed antenna. Lastly, in Fig. 7 (c), during the ON state at the frequency of 5.9 GHz, the beam shifts in the right direction. In the OFF state, the radiation pattern moves to 6 GHz, beginning to split the beam.

Next, in Fig. 8, the effect of the surface current is observed after placing the PIN diodes on the edges of the antenna to calculate the current density in the case of frequency at 4.7 GHz, where the PIN diode is ON and OFF. The total efficiency of the antenna with and without PIN diode is evaluated as demonstrated in Fig. 9 (a), The addition of the PIN diode increased resistive loss and introduced parasitic L/C components, along with bias circuit effects, which changed the antenna input impedance and resonant frequency. As a result, some of the input power was no longer radiated, the efficiency dropped from 70% to 64%, and the resonant frequency moved from 3.4 GHz to 4.7 GHz. Finally, the antenna performance in terms of S-parameters is validated with HFSS in addition of CST software as shown in Fig.9 (b), The slight difference in resonant frequency between HFSS and CST is scientifically expected, as each uses different numerical methods (FEM versus FIT or time domain), different meshing strategies, and default port and boundary settings. These factors slightly alter the actual electrical dimensions and impedance environment of the antenna in each simulation.

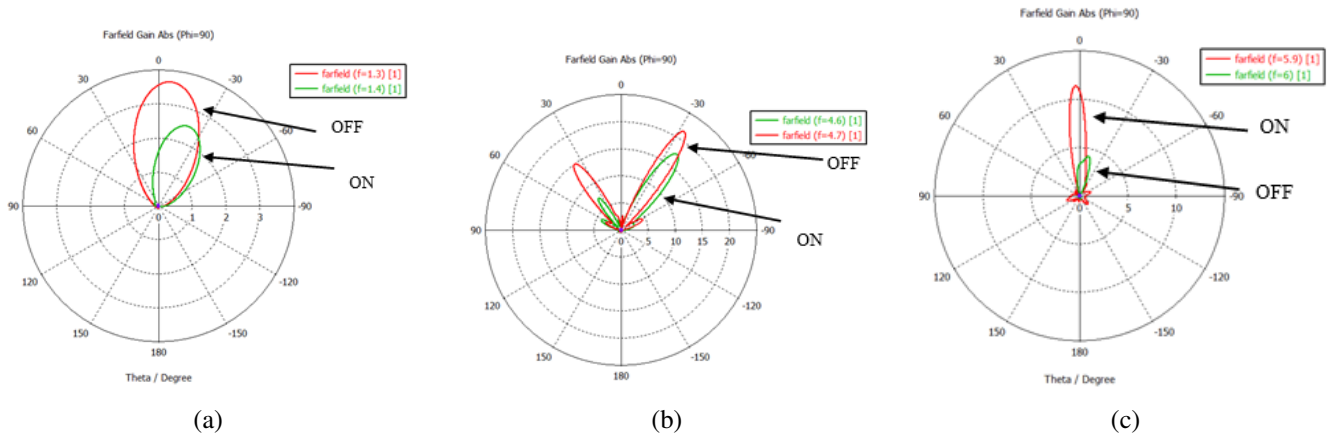


Figure 7: Radiation pattern results at frequencies (a) 1.3 and 1.4 GHz (b) 4.7 and 4.6 GHz (c) 5.9 and 6 GHz.

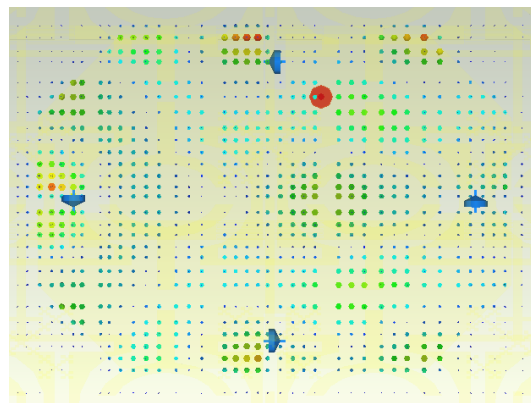


Figure 8: Surface current distributions at 4.7 GHz.

IV. COMPARISON WITH OTHER RELATED WORKS

The proposed antenna is compared with other studies in the literature in terms of peak gain, technique used, operating frequency, and reconfiguration type. As shown in Table III below, the comparison and the summary of the overall results of the antenna at different frequency resonances are given. Based on this comparison, it can be concluded that compared to other designs, this proposed antenna has higher gain and good impedance matching in addition to its low-profile construction, which guarantees multiple frequencies and polarizations with only a few PIN diodes required by the biasing system. The main contribution of this work is represented through its new design, which replaces the via with a fractal technique that lowers the capacitive losses of the via structure. It also uses four PIN diodes to increase the coupling with the MTM structure without changing the radiation pattern, which increases the gain and lowers the overall cost.

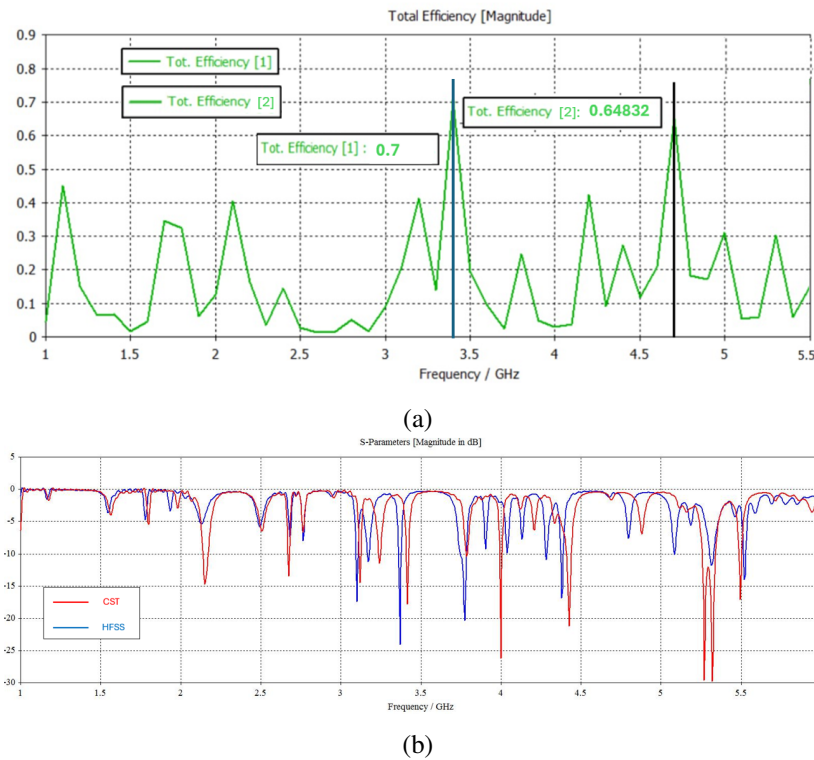


Figure 9: Simulation results of the proposed antenna (a) antenna efficiency with and without PIN diode (b) Reflection coefficient results using HFSS and CST.

TABLE III
Comparison between the proposed work and other related papers presented in the literature

Ref	Band Type	Resonance Frequency (GHz)	Bandwidth	Efficiency	Technique Used	Peak Gain (dBi)	Size (mm ²)	Applications
[19]	Dual-Band	5, 5.5	Not reported	Not reported	CRLH 16 pin	14.4	40 × 240	Long range communication
[20]	Multi-Band	1.57–2.15, 2.13–3.0, 3.17–3.43, 5.2–5.8, 6.3–6.78, 8.31–8.90	1.4–1.73, 4.75–5.72, 6.3–6.78, 8.31–8.90	Not reported	Omega / 2 pin	Not reported	77 × 135 × 0.6	Microwave sensing IoT applications
[8]	Dual	2.4, 5.8	2.41–2.47, 5.76–5.84	Not reported	Patch with EBG	6.6	113 × 113 × 9.6	Dual-band Wi-Fi & Access Points
[21]	Wide	2.76–8.21	2.76–8.21	80%	1 pin diode	5.8	35 × 25	Modern miniaturized wireless devices
[22]	Single	5.8	5.7298–5.8815	99.60%	Superstrate / patches / 2 pin	3.7	84 × 50	Dedicated Short Range Communication
[23]	Single	5.8	5.89–6.1	72.3%	Truncated square patch / 16 pin	11.9	70 × 70	Wireless communication
[17]	Wide	3.3–4.2, 4.86–5.98	3.3–4.2, 4.86–5.98	Not reported	CRLH / Hilbert EBG / 17 pin	3.74 / 7.24	40 × 240	Trucking systems (OFDM)
[24]	Multi-Band	2.1, 2.4, 3.5, 4.1, 4.8, 5.2	1.96–2.03	88%	L-shape MPA / 3 pin	3.26	33 × 6	WiMAX
This work	Multi-Band	2.1, 2.5, 2.6, 3.2, 3.7, 4.1, 5.2, 5.4, 5.6	1.5–5.6	65%	CRLH 4 pin	12.3	200 × 200	Long range communication

V. CONCLUSION

The research paper presents a flexible antenna design that can adapt to frequencies using multi-frequency pin diodes operating at 1.3 GHz, 4.7 GHz, and 5.9 GHz. The reflectance and pattern frequencies were calculated using CST software. The results demonstrate good gain and impedance matching for resonant frequencies, which are crucial for specific wireless applications. Furthermore, the antenna's features include its dimensions and complex geometric details achieved through openings that could influence its performance, which can be modified by the control provided by PIN devices. The simulated results indicate that the antenna can operate at three different frequencies with this gain increase. The antenna can be utilized in 5G applications.

This research model can be expanded to incorporate intelligent communication systems with automatic frequency adaptation in the Tera-Hertz (THz) bands of 6G communications technologies. The limited bandwidth in each operating mode and the sensitivity of the performance to variations in system impedance during switching processes are two issues with the current study. To improve performance while maintaining the structural characteristics of the antenna, future research suggests investigating hybrid metamaterial structures. It is also recommended to study the effects of thermal rise resulting from extended operation at high frequencies. These improvements would increase the effectiveness of the system and better suit it for communications applications that are dynamic and reconfigurable.

FUNDING

This work is funded by the UNITEN BOLD 2023 grant under the grant J510050976.

ACKNOWLEDGEMENT

The author would like to thank the reviewers for their valuable contribution in the publication of this paper.

CONFLICTS OF INTEREST

The author declares no conflict of interest.

REFERENCES

- [1] M. Y. Muhsin, F. M. Ali, A. J. Salim, Z. F. Mohammad, and J. K. Ali, "Comprehensive review of isolation techniques in MIMO antennas for 5G mobile devices," *News of higher educational institutions. Radioelectronics*, 2023.
- [2] B. Q. Elias, M. Alsajri, P. J. Soh, and A. A. Al-Hadi, "Design of flexible planar antennas using substrate gap structure for surface wave reduction," in *Proc. 22nd Int. Conf. Control Syst. Comput. Sci. (CSCS)*, Bucharest, Romania, 2019, pp. 453–458.
- [3] S. Kumar, *Wireless Communication—the Fundamental and Advanced Concepts*. Boca Raton, FL: CRC Press, 2022.
- [4] Y. Huo, X. Dong, and N. Ferdinand, "Distributed reconfigurable intelligent surfaces for energy-efficient indoor terahertz wireless communications," *IEEE Internet Things J.*, vol. 10, no. 3, pp. 2728–2742, 2022.
- [5] M. S. Rana, S. B. Rana, and M. M. Rahman, "Microstrip patch antennas for various applications: a review," *Indones. J. Electr. Eng. Comput. Sci.*, vol. 29, no. 3, pp. 1511–1519, 2023.
- [6] O. Ibrahim, T. Elwi, and N. Islam, "Gain enhancement of microstrip antennas using UC-PBG layer," *Can. J. Electr. Electron. Eng.*, vol. 3, no. 9, pp. 480–483, 2012.
- [7] N. Khalili Palandi, N. Nozhat, and R. Basiri, "Design and fabrication of small and low profile microstrip monopole antenna using CRLH-TL structures," *J. Electromagn. Waves Appl.*, vol. 33, no. 13, pp. 1749–1763, 2019.
- [8] M. F. Ismail et al., "Dual-band pattern reconfigurable antenna using electromagnetic band-gap structure," *AEU Int. J. Electron. Commun.*, vol. 130, p. 153571, 2021.
- [9] S. S. Behera and S. Sahu, "Frequency reconfigurable antenna inspired by metamaterial for WLAN and WiMAX application," in *Proc. Int. Conf. Signal Propag. Comput. Technol. (ICSPCT)*, 2014, pp. 442–446.
- [10] C. J. You et al., "Frequency and pattern reconfigurable antenna array with broadband tuning and wide scanning angle," *IEEE Trans. Antennas Propag.*, 2023.
- [11] H. Zhang, J. Yao, and T. Ni, "Compact CRLH-SIW based LWA array with periodical loading for Ku-band applications," *Prog. Electromagn. Res. Lett.*, vol. 108, pp. 59–64, 2023.
- [12] A. Kumar, B. Dewan, A. Khandelwal, and K. Shrivastava, "On the development of fractal antenna for IoT applications," *Eng. Res. Express*, vol. 5, no. 3, p. 035026, 2023.

- [13] K. Madhusudhana and S. P. Hegde, "Reconfigurable fractal microstrip antenna with varactor diode," *Global Transit.Proc.*, vol. 3, no. 1, pp. 183–189, 2022.
- [14] Y. M. Madany, "Multiband balanced CRLH-TL microstrip patch antenna for ultrawide band applications," in *Proc. Int. Telecommun. Conf. (ITC-Egypt)*, 2022, pp. 1–5.
- [15] G. A. Ramirez et al., "Reconfigurable dual-polarized beam-steering broadband antenna using a crossed-strips geometry," *IEEE Antennas Wireless Propag. Lett.*, vol. 20, no. 8, pp. 1379–1383, 2021.
- [16] B.-F. Zong, H.-Y. Zeng, F. Wu, G.-M. Wang, and L. Geng, "Wide-angle frequency-scanning array antenna using dual-layer finger connected interdigital capacitor based CRLH unit cell," *IEEE Access*, vol. 9, pp. 35957–35967, 2020.
- [17] M. M. Ismail, T. A. Elwi, and A. Salim, "A miniaturized printed circuit CRLH antenna-based Hilbert metamaterial array," *J. Commun. Softw. Syst.*, vol. 18, no. 3, pp. 236–243, 2022.
- [18] S. Sharma, R. Mehra, and S. Yadav, "Miniaturized circularly polarized broadband antenna based on CRLH-TL metamaterials for 5G millimeter-wave applications," in *Recent Trends Electron. Commun.: Sel. Proc. VCAS 2020*, 2022, pp. 963–971.
- [19] M. M. Ismail, T. A. Elwi, and A. J. Salim, "Reconfigurable composite right/left-handed transmission line antenna based Hilbert/Minkowski stepped impedance resonator for wireless applications," *Radioelectron. Comput. Syst.*, no. 1, pp. 77–91, 2023.
- [20] A. Vamseekrishna, B. T. P. Madhav, T. Anilkumar, and L. S. S. Reddy, "An IoT controlled octahedron frequency reconfigurable multiband antenna for microwave sensing applications," *IEEE Sensors Lett.*, vol. 3, no. 10, pp. 1–4, 2019.
- [21] N. Hussain, A. Ghaffar, S. I. Naqvi, A. Iftikhar, D. E. Anagnostou, and H. H. Tran, "A conformal frequency reconfigurable antenna with multiband and wideband characteristics," *Sensors*, vol. 22, no. 7, p. 2601, 2022.
- [22] W. I. Roseli, M. T. Ali, N. H. Abd Rahman, M. A. Aris, and H. Yon, "Performance enhancement of polarization reconfigurable antenna for wireless communication applications," in *Proc. Int. Symp. Antennas Propag. (ISAP)*, China, 2019, pp. 1–4.
- [23] B. Anantha, L. Merugu, and S. P. V. D. Rao, "Polarization reconfigurable corner truncated square microstrip array antenna," *IETE J. Res.*, vol. 67, no. 4, pp. 491–498, 2021. DOI: 10.1080/03772063.2018.1557084.
- [24] I. Shah, S. Hayat, A. Basir, M. Zada, S. Shah, and S. Ullah, "Design and analysis of a hexa-band frequency reconfigurable antenna for wireless communication," *AEU Int. J. Electron. Commun.*, vol. 98, pp. 80–88, 2019.